Journal of Science and Technology, Vol. 9 No. 3 (2017) p. 106-112

Sol-Gel Synthesis and Electrical Characterization of $Li_{1+x}Al_xTi_{2-x}(PO_4)_3$ Solid Electrolytes

Mohammed Isah Kimpa[1,2], Mohd Zul Hilmi Mayzan[1], Fahmiruddin Esa[1], Jibrin Alhaji Yabagi[1], Muhammad Muhammad Nmaya[1] and Mohd Arif Agam[1*]

[1]Materials Physics Laboratory (MPL), Faculty of Applied Sciences and Technology, Universiti Tun Hussein Onn Malaysia, Pagoh Campus, 84600 Pagoh, Muar, Johor, Malaysia.

[2]Department of Physics, School of Physical Sciences, Federal University of Technology Minna, P.M.B. 65, Minna, Niger State, Nigeria.

Received 30 September 2017; accepted 30 November 2017; available online 28 December 2017

Abstract: This composition of Lithium Aluminium Titanium Phosphate (LATP) has potential for the fast growing energy storage to be used as solid electrolyte in Li-ion battery. This material is required to solve safety problems of current lithium ion battery. In this study, $Li_{1+x}Al_xTi_{2-x}(PO_4)_3$ (x = 0.0, 0.1 and 0.2) nanocrystalline composition were synthesized by sol gel method. Lithium Nitrate ($LiNO_3$), Aluminium Nitrate Nonahydrate ($Al(NO_3)_3.9H_2O$), Titanium (IV) Butoxide ($Ti(OC_4H_9)_4$) and Ammonium dihydrogen phosphate ($NH_4H_2PO_4$) were used as starting materials. Citric acid monohydrate was used to control the pH value and ethylene glycol was used as solvent during the preparation. Pure NASICON-type powder with rhombohydral structure (*R-3c*) space group were obtained after heating the gel precursor at 950 °C for 5 h. The resulting materials were characterized using X-ray diffraction (XRD) and field emission scanning electron microscopy (FESEM). The Ionic conductivity of the polished samples was carried out using AGILENT 4294A precision impedance analyzer. The XRD analysis revealed pure crystalline phase of $LiTi_2(PO_4)_3$ NASICON structure with minor impurities (TiO_2 and TiP_2O_7). The highest ionic conductivity value was found approximately 7.936×10^{-4} S cm^{-1} for $Li_{1.2}Al_{0.2}Ti_{1.8}(PO_4)_3$ sample. It can be summarized that sol-gel method is more promising compared to traditional solid-state method.

Keywords: LATP, sol-gel method; electrolyte; ionic conductivity; NASICON.

1. Introduction

Lithium titanium phosphate $LiTi_2(PO_4)_3$ with NASICON-type structure has been well known as a solid electrolyte material for lithium ion battery [1–5]. This ceramics structure is known with high ionic conducting materials and are therefore potential solid electrolyte that could be used in batteries with high energy density ranging from portable electronic devices such as laptop, calculators to electrical vehicles [1,6,7].

Commercial lithium batteries available in recent years are mostly organic fluids as electrolyte. This problems causes leakages of the organic electrolyte and degradation of lithium ion battery. Thus, high lithium conducting solid electrolytes based on inorganic materials are strongly desired and have been investigated [8–11].

Properties of any materials generally depend on its purity and composition [12]. Several researchers synthesized NASICON-type systems [13] by conventional solid state method which required high temperatures [1,14,15]. The conventional method of heating the stoichiometric amounts of reactants at high temperatures leads to inhomogeneity, impurities, defects and large distribution in the particle size [16–18].

In contrast, the sol-gel method for the synthesis of lithium based solid electrolytes has demonstrated promising fabrication process due to several advantages during the preparation such as less time consuming, low reaction temperature and potentially yield high purity product [6,12].

Therefore, there is a systematic need for the synthesis of $LiTi_2(PO_4)_3$ ceramic through sol-gel method as an effective technique to prepare

*Corresponding author:arif@uthm.edu.my

NASICON composition material at lower temperatures. Sol-gel process involves obtaining a homogeneous sol of the material which undergoes thermal processes with rigorous mixture and resulted into a pure gel.

In this work, we investigate the effect of sol-gel method on Al doping and characterization of the resulting materials by using XRD, FTIR, FESEM and IS.

2. Experimental

The raw materials namely lithium nitrate ($LiNO_3$), aluminium nitrate nonahydrate ($Al(NO_3)_3{\cdot}9H_2O$), ammonium dihydrogen phosphate ($NH_4H_2PO_4$) were supplied by R & M except Titanium (IV) Butoxide ($Ti(OC_4H_9)_4$) by Sigma Aldrich. All chemicals were certified as analytical grade and used directly without any chemical treatments.

For the preparation of $Li_{1+x}Al_xTi_{2-x}(PO_4)_3$ with x = 0.0, 0.1 and 0.2, citric acid (CA) of 0.2 M aqueous solution was firstly dissolved in ethylene glycol (EG) to prepare the precursor solution. $Ti(OC_4H_9)_4$ was added and the solution was magnetically stirred at 120 °C for 8 h to increase homogeneity. CA is the complexion agent in the solution while EG acted as a polymer agent during a sol-gel process. The molar ratio of CA to EG was kept at 1:4. The calculated stoichiometric amounts of $LiNO_3$, $Al(NO_3)_3{\cdot}9H_2O$ and $NH_4H_2PO_4$ were slowly added into the above solution while stirring the mixtures for an hour without heating. The molar ratio of $Li^+ + Al^{3+} + Ti^{4+}$ to CA was set to meet the ratio of 1:2. The gel was dried in a MEMMERT drying oven for 4 h at 170 °C. The brown-colour xerogel was then calcined in PROTHERM chamber furnace at 500 °C for 4 hours with 5° C/min heating rate to complete the nitrates and organic compounds chemical decomposition. The heated sample was calcined for the second time at 800 °C for 2 h to obtain a whitish NASICON powder. Agate mortar and pestle was used to grind the calcined powder for 1 h to obtain a uniform fine powder. The fine powder was pressed into pellet using CARVER hydraulic pressing machine at 5 metric ton. A pellet of 13 mm diameter and 2-3 mm thickness were formed. The pelletized samples of different compositions were sintered at 950 °C for 5 h with 5 °C/min heating and cooling rates. The sintered pellets were grinded and polished to 1 µm before subjected to further characterization.

XRD measurements were performed on the sintered pellets to confirm the formation of crystalline structure and the phase transformations of the samples. The measurement was carried out using (Bruker D8 ADVANCE Powder X-ray Diffractometer) Cu Kα radiation source with λ = 1.5418 Å. The diffraction patterns were recorded at room temperature from 10 to 60º 2θ at step size of 0.02°. The XRD analysis was then conducted using X'Pert High Score Plus software package. FTIR spectrometer utilising PerkinElmer FTIR Spectrum software was used to identify the potential functional groups existing in LATP compositions. The microstructure analysis of selected samples were undertaken using JEOL JSM-7600F FESEM at 10 kV accelerating voltage. AGILENT 4294A precision impedance analyzer was used to investigate the electrical property of the sintered LATP pellets in a frequency range 40 Hz to 4 MHz at room temperature. Prior to impedance measurements, the polished LATP-x (x = 0.0, 0.1, 0.2) pellets were sandwiched between metal plates (16047E Dielectric Lead test fixture) as ionic blocking electrodes in order to ensure good electrical contact.

3. Results and Discussion

The crystalline phase information of LATP-x (x = 0.0, 0.1, 0.2) samples were characterized by XRD. The XRD patterns of all samples sintered at 950 °C for 5 h are shown in Fig. 1.

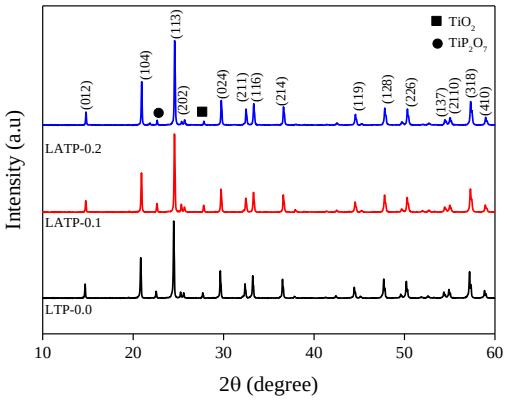

Fig. 1 XRD patterns of LATP-x samples sintered at 950 °C for 5 h.

According to the diffractograms, the dominant phase for all samples is $LiTi_2(PO_4)_3$ NASICON structure indexed with hexagonal

setting of the rhombohedra space group (S.G. *R-3c*). Very small amount of impurity phase TiO_2 and TiP_2O_7 can be observed from all sintered samples. These impurities could lead to the blocking of ionic pathway in the NASICON framework. However, impurity TiO_2 phase was due to loss of lithium at high temperature. Zhang et al claims that such impurity could appear for $LiTi_2(PO_4)_3$ compound due to loss of LiO_2 [19]. Using sol–gel method to synthesize $Li_{1+x}Al_xTi_{2-x}(PO_4)_3$ (x = 0.0, 0.1 and 0.2) nanocrystalline composition powders, the impurity peaks precipitated due to TiO_2 do occur in a samples prepared under high thermal treatment.

Fig. 2 shows the FTIR spectra of LATP-x (x = 0.0, 0.1, 0.2) measured from 2000 to 600 cm^{-1} wavenumbers. The band between 550 and 700 cm^{-1} is attributed to the asymmetric bending vibration mode of O−P−O unit [20]. The band between 975 to 965 cm^{-1} correspond to the symmetric stretching vibration of PO_4^{3-} ions [21–23]. The band between 1245 to 1225 cm^{-1} is assigned to PO_4 ionic vibration [21]. From the spectra, it can be seen that the bands at 970 cm^{-1} are broadening by partial substitution of Al^{3+} with Ti^{4+} for LATP-0.1 and LATP-0.2. This could be attributed to the cation substitution [24]. The occupancy of the cation in NASICON framework depends on the substituted Al^{3+} with Ti^{4+} within the structure. In $LiTi_2(PO_4)_3$ compound, the Li^+ ions are distributed in the M1 or M2 site with one atom each and $Ti^{4+}(Al^{3+})$ are randomly distributed [25]. In addition, the band located between 1245 and 1225 cm^{-1} diminished with the increasing of Al content. This might be due to the effects of thermal treatment during sintering. Similar result was reported for higher sintering effect by [26].

Fig. 3 shows the top surface and cross-section FESEM images of all sintered pellets. It is clear that all samples having faceted and rectangular cubic structure. This is in agreement with other study that reported near identical morphology of NASICON structure [6,27]. There is significant grain growth for Al substitution samples which reduced the porosity of the sintered pellet to allow ion percolation across the grain boundaries for LATP-0.2 sample.

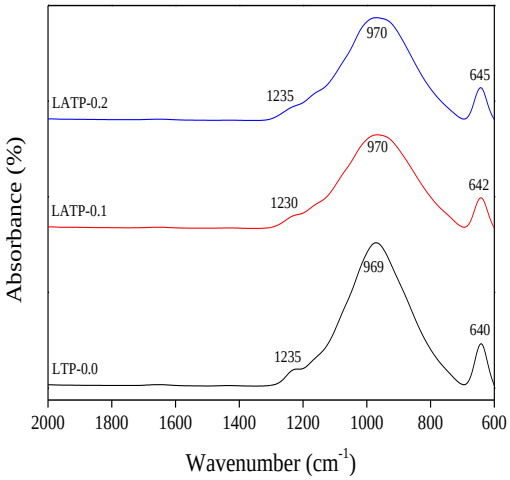

Fig. 2 FTIR Spectra of LATP-x (x = 0.0, 0.1, 0.2) samples.

Fig. 4 show the electrical characterization of the complex impedance plot for LATP-x (x = 0.0, 0.1, 0.2) samples sintered at 950 °C for 5 h. The measurement was performed at room temperature from frequency ranges of 40 Hz to 4 MHz. The frequency increased from right to left along the impedance curves because impedance is a function of frequency dependence. From the Nyquist plot, it was observed that the impedance plots for all samples had similar trend. In principle, semicircle was observed at high frequency region which indicates bulk contribution to conductivity while a spike (straight slanted line) was observed at low frequency region due to the electrode-ceramics polarization. In a device, the important measure for practical application is the total Li-ion conductivity rather than bulk Li-ion conductivity.

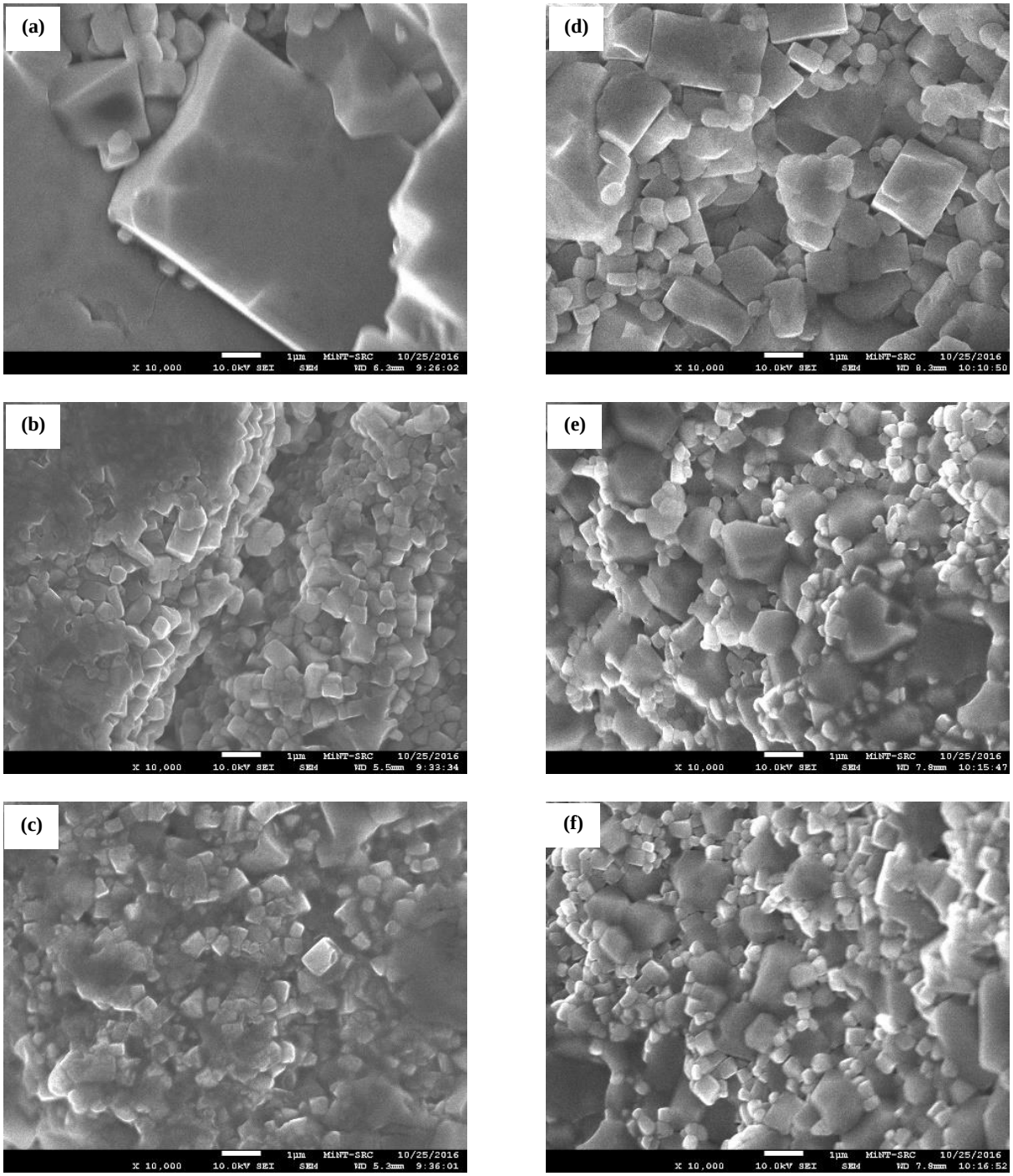

Fig. 3 FESEM micrographs of LATP-*x* (*x* = 0.0, 0.1, 0.2) samples sintered at 950 °C for 2 h, (a-c) top surface and (d-f) cross-section

.

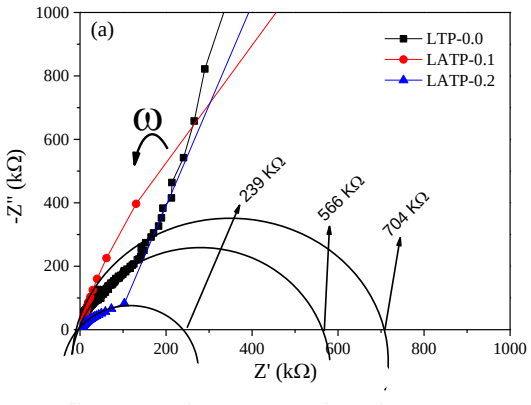

Fig. 4 Complex impedance plot for LATP-*x* (*x* = 0.0, 0.1, 0.2) sample.

In this study, the overall total ac conductivity for LTP-0.0, LATP-0.1 and LATP-0.2 were calculated using the relation given in Eq. 1.

$$\sigma_{ac} = \frac{dG}{A} \qquad (1)$$

where, *d* is thickness of sample, *A* is area of electrodes used and *G* is conductance of sample.

The lack of clear semicircles at higher frequency region is due to the materials having low grain boundary impedance. This statement is in agreement with recent studies of which suggested that the lack of clear semicircles at the highest frequencies regions is an indication of negligible grain boundary resistance [28,29]. At higher temperatures, the semicircle shifts out of the frequency window, and thus only the total resistance of the sample can be determined [30]. The intersect values of semicircle at *x*-axis obtained for each sample (see Fig. 4) indicate the magnitude of the radius tends to decrease with the increasing of Al content; from LTP-0.0 to LATP-0.2. Decreasing radius of the semicircle implies higher conductivity value [31].

The total resistance of the NASICON ceramics was determined from the intercept of electrode and grain-boundary arcs with the real axis as shown in Fig. 4.

The real part, *Z'(ω)* and the imaginary part, *Z''(ω)*, of complex impedance *Z*(ω) = Z'(ω) – jZ''(ω)*, are related to measured Conductance, *G* and Capacitance, *C* values as follows:

$$Z'(\omega) = \frac{G}{\left(G^2 + C^2\omega^2\right)} \quad and \quad Z'' = \frac{C\omega}{\left(G^2 + C^2\omega^2\right)} \qquad (2)$$

The ac conductivity of LTP-0.0, LATP-0.1 and LATP-0.2 samples were 1.367×10^{-5} S/m, 1.132×10^{-4} S/m and 7.936×10^{-4} S/m respectively. This indicates the conductivity is greatly improved when the material is partially substituted with Al content; the conductivity increases by one order of magnitude for LATP-0.2 sample.

4. Conclusion

LATP-*x* (*x* = 0.0, 0.1, 0.2) have been successfully prepared via sol-gel method and sintered at 950 °C for 5 h. XRD data shows a pure NASICON phase with small amount of impurity phase TiO_2 and TiP_2O_7 observed from all sintered samples which was due to loss of lithium during high thermal treatment. Increasing the Al content resulted into increase of ac conductivity (σ_{ac}) by one order of magnitude from 1.367x 10^{-5} for undoped LTP to 7.936x10^{-4} S/m for Al doped sample (LATP-0.2). Based on this study, LATP solid electrolyte prepared using sol-gel method make it easy to synthesized homogeneous precursor solution at a considerably low temperature for a short synthesis time compared to traditional solid-state reaction methods. The high conductivity, good chemical stability and easy fabrication of this method provide a promising candidate as a solid electrolyte for all-solid-state lithium ion rechargeable batteries.

Acknowledgement

The authors are grateful to UTHM and Federal University of Technology Minna Nigeria for their encouragement and support. This research work is funded under incentive for publication grant (IGSP), U412 as well as graduate research incentive grant (GIPS), U301.

References

[1] Lin-chao, Z., Chen, P., Hu, Z. & Chen, C (2012). "Electrical properties of NASICON-type structured $Li_{1.3}Al_{0.3}Ti_{1.7}(PO_4)_3$ solid electrolyte prepared by 1,2-propylene glycol-assisted sol-gel method" in Chinese Journal of Chemical Physics, Vol. 25.

No. 6 pp. 703–707.

[2] Dokko, K., Hoshina, K., Nakano, H. & Kanamura, K (2007). "Preparation of $LiMn_2O_4$ thin-film electrode on $Li_{1+x}Al_xTi_{2-x}(PO_4)_3$ NASICON-type solid electrolyte" in Journal of Power Sources, Vol. 174, No. 2 pp. 1100–1103.

[3] Monchak, M., Hupfer, T., Senyshyn, A., Boysen, H., Chernyshov, D., Hansen, T., Schell, K.G., Bucharsky, E.C., Hoffmann, M.J. & Ehrenberg, H (2016). "Lithium diffusion pathway in $Li_{1.3}Al_{0.3}Ti_{1.7}(PO_4)_3$ (LATP) superionic conductor" in Inorganic Chemistry, Vol. 55. No. 6 pp. 2941–2945.

[4] El-Shinawi, H. and Janek, J. (2015). "Low-temperature synthesis of macroporous $LiTi_2(PO_4)_3$/C with superior lithium storage properties" in RSC Adv, Vol. 5. No. 19 pp. 14887–14891.

[5] Kotobuki, M., Isshiki, Y., Munakata, H. & Kanamura, K. (2010). "All solid state lithium battery with a three dimensionally ordered $Li_{1.5}Al_{0.5}Ti_{1.5}(PO_4)_3$ electrode" in Electrochimica Acta, Vol. 55. No. 22 pp. 6892–6896.

[6] Xu, X., Wen, Z., Wu, J. and Yang, X (2007). "Preparation and electrical properties of NASICON-type structured $Li_{1.4}Al_{0.4}Ti_{1.6}(PO_4)_3$ glass-ceramics by the citric acid-assisted sol-gel method" in Solid State Ionics, Vol. 178. No. 1–2 pp. 29–34.

[7] Gao, Y. X., Wang, X. P., Wang, W. G. & Fang, Q. F (2010). "Sol–gel synthesis and electrical properties of $Li_5La_3Ta_2O_{12}$ lithium ionic conductors" in Solid State Ionics, Vol. 181. No. 1–2 pp. 33–36.

[8] Zhang, M., Takahashi, K., Uechi, I., Takeda, Y., Yamamoto, O., Im, D., Lee, D.J., Chi, B., Pu, J., Li, J. & Imanishi, N. (2013). "Water-stable lithium anode with $Li_{1.4}Al_{0.4}Ge_{1.6}(PO_4)_3$-$TiO_2$ sheet prepared by tape casting method for lithium-air batteries" in Journal of Power Sources, Vol. 235 pp. 117–121.

[9] Capsoni, D., Bini, M., Ferrari, S., Mustarelli, P., Massarotti, V., Mozzati, M.C. & Spinella, A. (2010). "Structural, spectroscopic and electrical features of undoped and Mn-Doped $LiTi_2(PO_4)_3$" in Journal of Physical Chemistry C, Vol. 114. No. 32 pp. 13872–13878.

[10] Xiao, Z., Chen, S. & Guo, M (2011). "Influence of Li_3PO_4 addition on properties of lithium ion-conductive electrolyte $Li_{1.3}Al_{0.3}Ti_{1.7}(PO_4)_3$" in Transactions of Nonferrous Metals Society of China, Vol. 21. No. 11 pp. 2454–2458.

[11] Ortiz, G.F., López, M.C., Lavela, P., Vidal-Abarca, C. & Tirado, J.L (2014). "Improved lithium-ion transport in NASICON-type lithium titanium phosphate by calcium and iron doping" in Solid State Ionics, Vol. 262 pp. 573–577.

[12] Navulla, A (2010). "Semi sol–gel synthesis, conductivity and luminescence studies of $Ca_{0.5}Fe_{1-x}Eu_xSb(PO_4)_3$ (x=0.1, 0.15 and 0.2)" in Solid State Ionics, Vol. 181. No. 13–14 pp. 659–663.

[13] Wang, Y.J., Pan, Y. & Kim, D. (2006) "Conductivity studies on ceramic $Li_{1.3}Al_{0.3}Ti_{1.7}(PO_4)_3$-filled PEO-based solid composite polymer electrolytes" in Journal of Power Sources, Vol. 159. No. 1 pp. 690–701.

[14] Arbi, K., Kuhn, A., Sanz, J. & García-Alvarado, F (2010). "Characterization of Lithium Insertion into NASICON-Type $Li_{1+x}Ti_{2-x}Al_x(PO_4)_3$ and Its Electrochemical Behavior" in Journal of The Electrochemical Society, Vol. 157. No. 6 pp. A654–A659.

[15] Rusdi, H., Abd Rahman, A., Subban, R.H.Y. & Mohamed, N.S (2012). "Characterisation of Lithium Aluminium Titanium Phosphate as Solid Electrolytes Synthesized by Mechanical Milling Method" in Advanced Materials Research, Vol. 545 pp. 190–194.

[16] Pérez-Estébanez, M., Isasi-Marín, J., Rivera-Calzada, A., León, C. & Nygren, M (2015). "Spark plasma versus conventional sintering in the electrical properties of Nasicon-type materials" in Journal of Alloys and Compounds, Vol. 651 pp. 636–642.

[17] Alias, R (2013). "Structural and Dielectric Properties of Glass-Ceramic Substrate with Varied Sintering Temperatures" in Materials Science: Sintering Applications, pp. 90–118.

[18] Yadav, P & Bhatnagar, M.C (2012). "Structural studies of NASICON material of different compositions by sol-gel method" in Ceramics International, Vol. 38. No. 2 pp. 1731–1735.

[19] Zhang, M., Takahashi, K., Imanishi, N., Takeda, Y., Yamamoto, O., Chi, B., Pu, J. & Li, J (2012). "Preparation and Electrochemical Properties of $Li_{1+x}Al_xGe_{2-x}(PO_4)_3$ Synthesized by a Sol-Gel Method" in Journal of The Electrochemical Society, Vol. 159159. No. 776 pp. 1114 –1119.

[20] Tan, G., Wu, F., Li, L., Liu, Y. & Chen, R (2012). "Magnetron sputtering preparation of nitrogen-incorporated lithium-aluminum-titanium phosphate based thin film electrolytes for all-solid-state lithium ion batteries" in Journal of Physical Chemistry C, Vol. 116. No. 5 pp. 3817–3826.

[21] Vinoth Rathan, S. & Govindaraj, G (2010). "Thermal and electrical relaxation studies in $Li_{(4+x)}Ti_xNb_{1-x}P_3O_{12}$ ($0.0 \leq x \leq 1.0$) phosphate glasses" in Solid State Sciences, Vol. 12. No. 5 pp. 730–735.

[22] Savitha, T., Selvasekarapandian, S. and Ramya, C.S (2008). "Structural and electrical conductivity studies of $LixAlZr[PO_4]_3$ (x = 1.8, 2.0, 2.2), solid electrolyte for lithium-rechargeable batteries" in Journal of Solid State Electrochemistry, Vol. 12. No. 7–8 pp. 857–860.

[23] Mustaffa, N.A., Adnan, S.B.R.S., Sulaiman, M. & Mohamed, N.S (2014). "Low-temperature sintering effects on NASICON-structured $LiSn_2P_3O_{12}$ solid electrolytes prepared via citric acid-assisted sol-gel method" in Ionics, Vol. 21. No. 4 pp. 955–965.

[24] Hamidi, M.B (2014). Preparation and Characterization of Lithium Based Glass Ceramic Conducting Electrolytes, Universiti Teknologi Mara,

[25] Antony, C.J., Aatiq, A., Panicker, C.Y., Bushiri, M.J., Varghese, H.T. & Manojkumar, T.K (2011). "FT-IR and FT-Raman study of Nasicon type phosphates, $ASnFe(PO_4)_3$ [A = Na_2, Ca, Cd]" in Spectrochimica Acta - Part A: Molecular and Biomolecular Spectroscopy, Vol. 78. No. 1 pp. 415–419.

[26] Biao, W., Xi-shuang, L., Feng-min, L.I.U., Tie-gang, Z., Chun, Z., Ge-yu, L.U. & Bao-fu, Q (2009). "Synthesis and characterization of NASICON nanoparticles by sol-gel method" in Chem Res Chinese Universities, Vol. 25. No. 3 pp. 13–16.

[27] Chang, C.M., Il Lee, Y., Hong, S.H. & Park, H.M (2005). "Spark Plasma Sintering of $LiTi_2(PO_4)_3$-Based Solid Electrolytes" in Journal of the American Ceramic Society, vol. 88, no. 7, pp. 1803–1807.

[28] Allen, J. L., Wolfenstine, J., Rangasamy, E. & Sakamoto, J (2012). "Effect of substitution (Ta, Al, Ga) on the conductivity of $Li_7La_3Zr_2O_{12}$," in Journal of Power Sources, Vol. 206. pp. 315–319.

[29] Kotobuki, M., Hoshina, K. & Kanamura, K (2011). "Electrochemical properties of thin TiO_2 electrode on $Li_{1+x}Al_xGe_{2-x}(PO_4)_3$ solid electrolyte" in Solid State Ionics, Vol. 198. No. 1 pp. 22–25.

[30] Mariappan, C.R., Gellert, M., Yada, C., Rosciano, F. & Roling, B (2012). "Grain boundary resistance of fast lithium ion conductors: Comparison between a lithium-ion conductive Li-Al-Ti-P-O-type glass ceramic and a $Li_{1.5}Al_{0.5}Ge_{1.5}P_3O_{12}$ ceramic" in Electrochemistry Communications, Vol. 14. No. 1 pp. 25–28.

[31] Ji-Sun, L., Chang, C.M., Il Lee, Y., Lee, J.H. & Hong, S.H (2004). "Spark Plasma Sintering (SPS) of NASICON Ceramics" in Journal of the American Ceramic Society, Vol. 87. No. 2 pp. 305–307.